Proceedings World Geothermal Congress 2020+1
Reykjavik, Iceland, April - October 2021

A Probabilistic Geologic Model of the Krafla Geothermal System Based on Bayesian Inversion of Gravimetric Data

Samuel Scott, Cari Covell, Egill Juliusson, Águst Valfells, Juliet Newson, Birgir Hrafnkelsson, Halldór Pálsson, María Gudjónsdóttir

School of Engineering, Reykjavik University, Menntavegur 1, 105 Reykjavik, Iceland

samuels@ru.is

Keywords: geologic modeling, Bayesian inference, gravity, geophysical inversion, Krafla

ABSTRACT

The quantitative connections between subsurface geologic structure and measured geophysical data allow 3D geologic models to be tested against measurements and geophysical anomalies to be interpreted in terms of geologic structure. However, geologic models are built on sparse and uncertain data, and the non-uniqueness of geophysical data implies that an infinite number of realizations of subsurface structure may be consistent with geophysical measurements. Bayesian inversion of gravity data accounts for the inherent uncertainty of gravity data by describing the inferred lithologic and mass density structure in terms of posterior probability distributions. Such methods require the specification of a prior model of subsurface structure and rock properties. It is challenging to select the probabilistic weights and the structure of the prior model in such a way that the inversion process retains relevant geologic insights from the prior while also exploring the full range of plausible subsurface models. In this study, we investigate how the uncertainty of the prior controls the inferred lithologic and mass density structure obtained by probabilistic inversion of gravimetric data measured at the Krafla geothermal system. We combine a reference prior geologic model with statistics for rock properties (grain density and porosity) in a Bayesian inference framework implemented in the GeoModeller software package. The uncertainty of the reference prior geologic model controls exerts a strong control on the inferred lithologic structure, mass density distribution, and uncertainty quantification metrics. By assuming a moderate uncertainty of the prior, the posterior lithologic structure deviates from the reference prior model in areas where it may be most likely to be inconsistent with the observed gravity data. In the case of Krafla, we observe this deviation in the vicinity of Leirbotnar sub-field, and investigate whether the discrepancy may be resolved by including a low density intrusion to the reference geologic model or by accounting for the effects of alteration in the assumed prior properties of hyaloclastite. This study underscores the importance of reliable prior constraints on lithologic structure and rock bulk density during Bayesian inversion of gravity data.

1. INTRODUCTION

Geophysical measurements can be used to test existing geologic models and infer the properties of the subsurface in areas where primary data (e.g., from boreholes) is not available. If primary data is available, thus given a prior model of the subsurface, inversion improves the correspondence between measured data and the calculated geophysical data (reduces the misfit) by adjusting the structure and properties of that model. Deterministic inversion methods calculate a solution that minimizes this misfit by modifying only the physical properties of the model cells specified in the initial model (Li and Oldenburg, 1998) and/or by modifying the rock type (and indirectly, the physical properties) of the model cells (Fullagar et al., 2008). As inversion of gravity potential field data is highly under-constrained (a phenomenon termed non-uniqueness in geophysical inverse theory), the *a priori* constraints on the geometric arrangement of the main rock units and their petrophysical properties in the initial model play a critical role in retaining geological meaning in the inversion process (Li and Oldenburg, 1998; Boulanger and Chouteau, 2001). Manual adjustment of the initial model geometry and/or rock properties is typically performed to assess how the uncertainty of the geometry of the initial model itself and the physical properties of each rock type affect the inversion (e.g., Abdelfettah et al., 2014; Altwegg et al., 2015; Witter et al., 2016; Miller et al., 2017).

Probabilistic inversion methods are becoming increasingly popular as geologic modeling becomes integrated into advanced machine-learning and Bayesian inference frameworks (Calcagno et al., 2008; Jessell et al., 2014; de la Varga et al., 2019).These techniques generate millions of possible realizations of subsurface structure from a reference prior model by stochastically varying lithologic structure and rock physical properties according to specified prior probability distributions. Similar to deterministic techniques, a geologic model configuration is considered more likely if it is consistent with prior geologic information about the system and it reduces the misfit between the forward-modeled geophysical field with measured data. However, in contrast to deterministic inversion techniques, such approaches provide posterior probability distributions for rock type and corresponding rock properties over the model space (Bosch, 1999; Bosch et al., 2001; Guillen et al., 2008; Chen et al., 2012; Jessell et al., 2014; McCalman et al., 2014; Corbel and Wellmann, 2015; de la Varga et al., 2015; Wellmann et al., 2017).

The non-uniqueness of gravity potential field data means that an infinite number of possible realizations of the subsurface density structure may be consistent with measured data. This partially makes Bayesian inference methods well-suited for the inversion of gravity potential field data, since they allow a prior model of the distribution of rock types and density to reflect the additional knowledge gained about the subsurface through the gravity data. The prior beliefs are updated based on a likelihood probability, which describes a probabilistic relationship between model and data and is based on knowledge of physical laws and measurement error. Although the uncertainty of the gravity data may be significant, the more difficult uncertainty to account for in Bayesian inversion of geophysical data is the uncertainty of the prior (e.g., Scales and Tenorio, 2001; Caers, 2011). While an overly conservative prior will restrict the possible solution space and lead to underestimation of uncertainty, an overly broad prior will produce geologically meaningless results.

In this study, we develop a probabilistic geologic model of the Krafla geothermal field constrained by gravimetric data. Our approach combines 3D geologic modeling, statistical analyses of rock properties, and inversion of gravimetric data to assess the lithologic and density structure of a volcanic geothermal system. The Bayesian inference framework implemented in GeoModeller V4 (Intrepid Geophysics, 2017a, 2017b) uses Markov Chain Monte Carlo sampling to calculate the posterior probability densities for the model parameters lithology and bulk density in light of the observed gravity data. We incorporate two forms of empirical prior information about the Krafla system, a reference geological model developed by expert geologists (Mortensen et al., 2009; Weisenberger et al., 2015), and probability distributions describing the bulk mass densities of the main rock types based on statistical analyses of laboratory measurements. Our main objective is to assess how treatment of uncertainty in the reference prior geologic model and petrophysical properties affects the probabilistic inversion results. We formulate the expected overlap between posterior results and the reference prior model probabilistically, in terms of the commonality criterion. In addition, we vary the structure of the reference prior model and the prior physical properties of the main rock types. This study shows that the uncertainty of the prior exerts a strong control on the uncertainty of posterior results obtained by Bayesian inversion of gravimetric data.

2. METHODOLOGY

Our approach combines a reference prior geologic model of Krafla built from borehole data (Weisenberger et al., 2015), measured gravimetric data (Magnusson, 2016) and statistics for rock petrophysical properties (Franzson et al., 2001, 2010, 2011; Frolova et al., 2005) within a Bayesian inference scheme implemented in the geologic modeling package GeoModeller (GeoModeller, 2017a, 2017b).

2.1 Geologic and Geophysical Data from the Krafla Geothermal System

Krafla is one of five active volcanic centers arranged in en-echelon fashion within the northern volcanic zone (NVZ) in northeast Iceland (Figure 1). The Krafla area features a volcanic caldera astride a major NNE-SSW trending fissure swarm (Saemundsson, 2008). The subsurface geology mainly consists of alternating layers of sub- or intra-glacially erupted basaltic hyaloclastite (a broad term describing highly heterogeneous rocks consisting of a mix of breccias, tuffs and pillow basalts) and subaerially-erupted basaltic lava flows in the upper ~1.5 km, with interspersed basaltic dike and sills and rhyolitic intrusions. Doleritic and gabbroic intrusions become increasingly pervasive below 1.5 km depth, along with minor granophyre and other silicic intrusions.

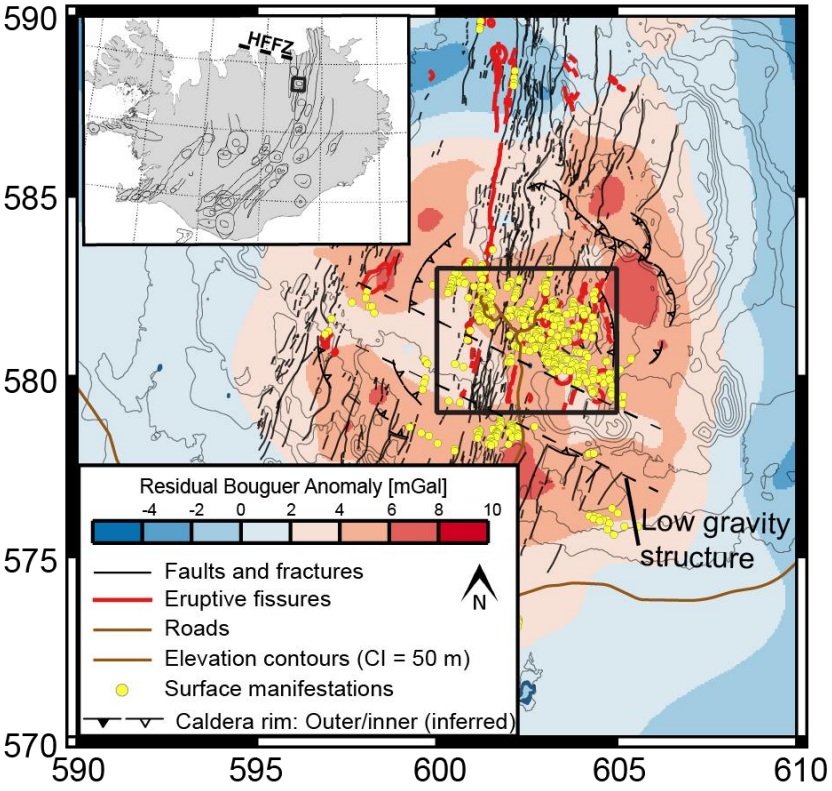

Figure 1. Topographic map of the Krafla area showing Residual Bouguer anomaly, geothermal surface manifestations, eruptive fissures and craters, outer caldera rim, inferred inner caldera rim and roads. Dashed lines show boundary of low gravity structure. Box shows the area of the geologic model built in this study. Coordinates are shown in ISNET95 (same as Lambert 95). Inset shows the location of Krafla geothermal system in NE Iceland, outline of rift zones and active volcanic centers, and Husavik-Flatey Fracture zone (HFFZ).

Several gravity surveys were carried out at Krafla between 1969-2015 (Johnsen et al., 1980; Johnsen et al., 1995; Magnusson, 2016). The gravity data used in this study is described in detail by Magnusson (2016), which considers 522 measurements made over an area of ~625 km^2. Station spacing is highly variable, ranging from 0.1 km to ~10 km, with a total of 49 stations located within the 20 km^2 area of the geologic model. Following Magnusson (2016), the residual Bouguer anomaly is calculated by subtracting the regional

field, estimated by fitting a third-degree polynomial trend to longer-wavelength signals, from the Bouguer anomaly, which is calculated assuming a reference density of 2.51 g cm^{-3}, consistent with Magnusson (2016). The residual Bouguer anomaly shown in Figure 2c reveals high gravity anomalies near the outer caldera rims of the Krafla volcano. Based on the transition between high gravity anomalies near the outer caldera rims and lower gravity values in the center of the central volcano, Árnason et al. (2007) inferred the existence of an inner caldera, containing a greater thickness of low-density hyaloclastites, buried within the outer caldera. The gravity data also show a WNW-ESE trending gravity low (shown with dashed lines in Figure 1) that transects the center of the caldera. Árnason et al. (2007) postulated that the WNW-ESE trending gravity low represents an oblique transform graben containing a greater thickness of hyaloclastite. The existence of thicker hyaloclastite layers in the south is supported by geologic data from boreholes that show the depth of basement decreases from Leirbotnar near the central part of the field to Hvitholar in the south (Ármannson et al., 1987).

A reference prior geologic model of the Krafla system was developed based on surface geologic mapping (Saemundsson, 2008) and an interpreted 3D geologic model for the system previously built in Petrel (Mortensen et al., 2009; Weisenberger et al., 2015). Figure 2 shows the surface geology within the model domain (the area of which is shown inside the white box in Figure 1) as well as the location of cross-sections shown in Figures 2b-d. The reference geologic model presents a simplified interpretation of the complex sequence of lithologic units identified from well cuttings (Mortensen et al., 2009 and references therein). The eleven stratigraphic units consist of an alternating sequence of five lava flow units (L1-L5, shown in blue) and four hyaloclastite units (H1-H4, yellow) underlain by basement intrusions (B, red) and overlain in some areas by a thin (<0.2 km) surface cover (grey). Although the total area of the reference prior geologic model is 25 km^2, most of the wellbore data, upon which the geologic model is based, is derived from a smaller area in the center of the model (wellbore locations shown by the black dots in Fig. 2a).

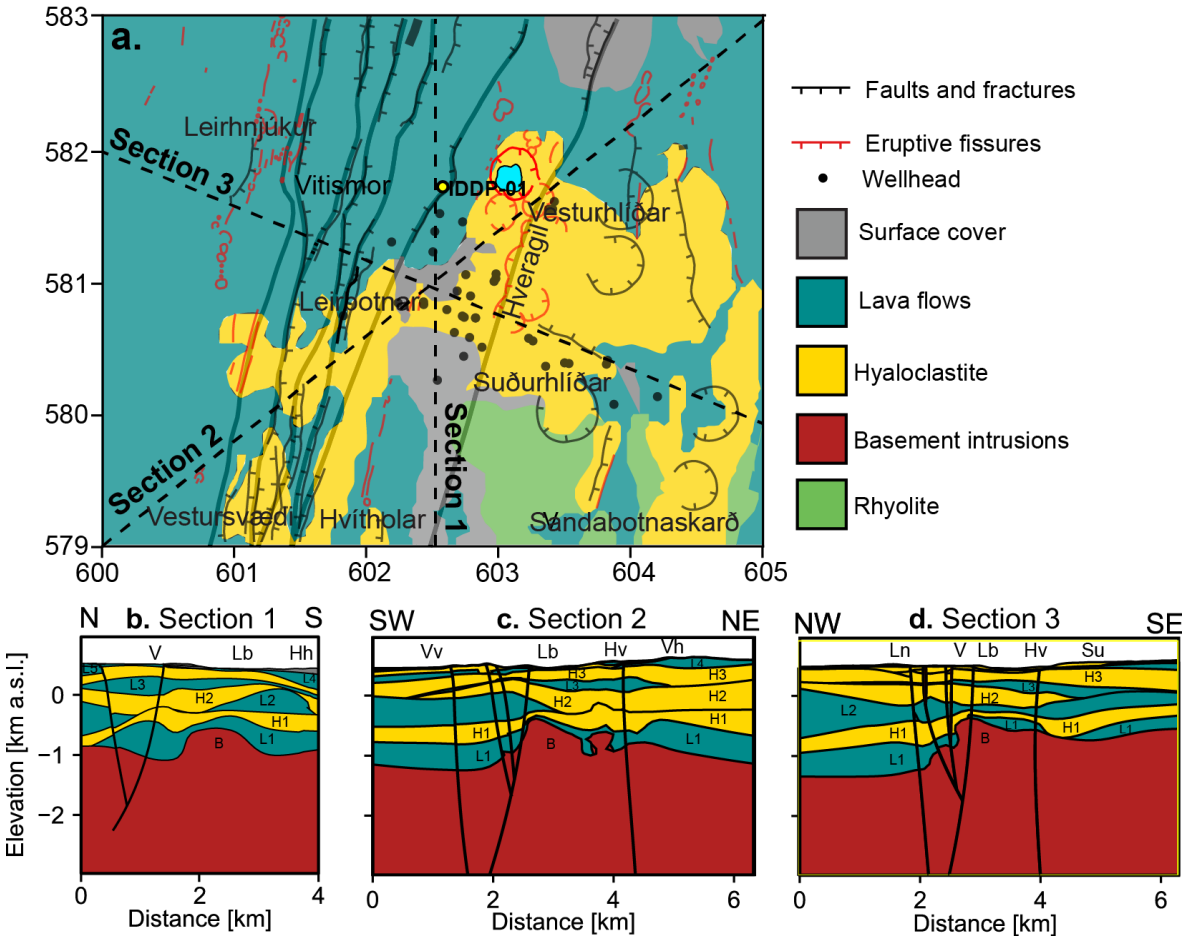

Figure 2. Reference geologic model of the Krafla system. a. Surface geologic map of Krafla caldera, showing mapped faults and fractures (black), inferred fault network (grey), eruptive fissures (red), and locations of wells (black dots), as well as the surface traces of b. Section 1 (N-S), c. Section 2 (SW-NE), and d. Section 3 (NW-SE).

2.2 Rock properties

Statistics for grain density and total porosity of the main lithologic units were derived as part of compilation of the Valgardur database, compiled from previous studies of Icelandic rock properties (Franzson et al., 2001, 2010, 2011; Frolova et al., 2005). Based on the rock descriptions, the samples were grouped into three lithologic types: 1) hyaloclastite, encompassing sub-glacially erupted breccias, tuffs, and pillow basalts, 2) sub-aerially erupted basaltic lavas, 3) basement intrusions, including doleritic dykes and sills crystallized at depth as well as gabbroic intrusions. The measured data for grain density and total porosity are shown in Figure 3a. Hyaloclastites have a slightly lower grain density (2.69 ± 0.13 g cm^{-3}) than the lava flows (2.87 ± 0.11 g cm^{-3}) and basement intrusions (2.75 ± 0.18 g cm^{-3}). However, the porosity of hyaloclastites is much higher (0.25 ± 0.14) compared to lava flows and basement intrusions (0.8 ± 0.1 and 0.03 ± 0.04, respectively). The statistics for grain density and porosity were used to calculate bulk wet density based on the

mass-weighted contributions of the solid rock matrix and fluid in the pore space. Normal and beta distributions were fitted to measured grain density and total porosity, respectively. The prior probability density functions (pdfs) for the bulk density for each rock type (Fig. 3b) were calculated by Monte Carlo sampling of the the pdfs for grain density and total porosity and assumption of a constant fluid density of 0.8 g cm^{-3} (corresponding to ~250 °C pure water). The bulk density of hyaloclastite (2.10 ± 0.36 g cm^{-3}) is much lower than lava flows (2.65 ± 0.24 g cm^{-3}) or basement intrusions (2.73 ± 0.14 g cm^{-3}), reflecting the high porosity of hyaloclastites. The thin surface cover (<0.2 km thick) was assigned a bulk density equal to the reference density used in calculation of the Bouguer anomaly (2.51 ± 0.10 g cm^{-3}).

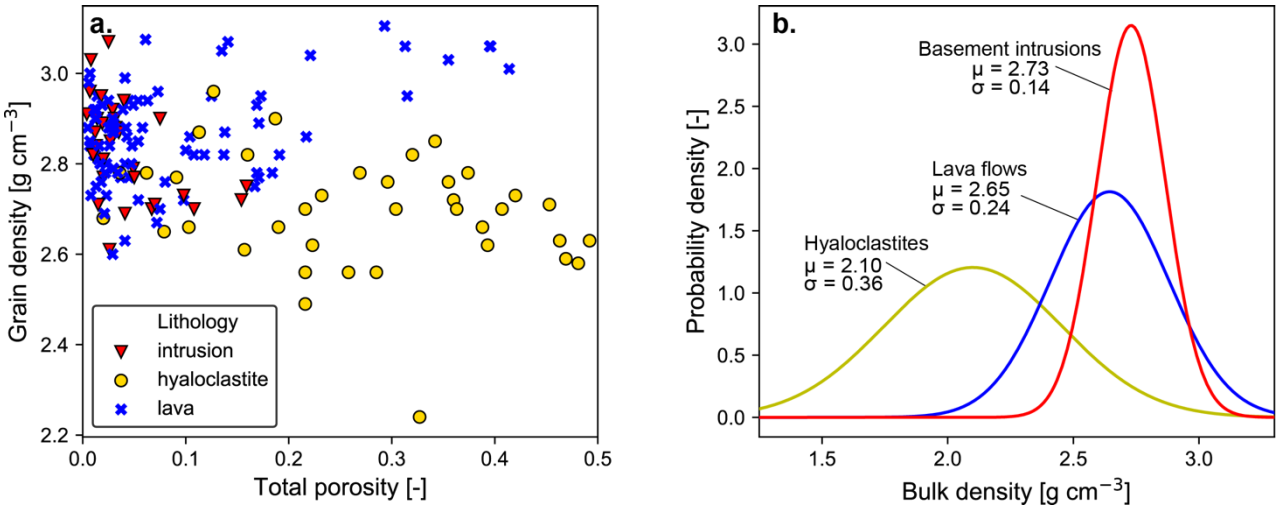

Figure 3. Rock property data. a. Measured data from the Valgardur database for grain density and total porosity, sorted by lithology. b. Prior probability distribution functions (pdfs) for bulk (wet) density obtained through Monte Carlo sampling.

2.3 Bayesian inference framework

GeoModeller uses a Markov Chain Monte Carlo (MCMC) statistical sampling scheme to drive the litho-constrained 3D inversion process and evaluate the posterior probability distribution. The method has been described previously in detail (Bosch, 1999; Bosch et al., 2001; Guillen et al., 2008) and will therefore only be briefly summarized here. The Bayesian inference scheme divides the prior probability space into a primary geologic parameter space ($\mathbf{m}_{\mathbf{pri}}$) describing the spatial distribution of the lithologies and a secondary parameter space ($\mathbf{m}_{\mathbf{sec}}$) describing rock petrophysical properties conditional on lithology. Measurements of the gravity potential field, denoted by y, constitute the additional information about the system which is used to infer lithology and density structure throughout the model domain through their the posterior probability density function which, according to a Bayes' law, is given by:

$$\pi\left(\mathbf{m}_{\text{sec}}, \mathbf{m}_{pri} \middle| y\right) = cL(y|\mathbf{m}_{\text{sec}})\pi_{s|p}(\mathbf{m}_{\text{sec}}|\mathbf{m}_{pri})\pi_{p}(\mathbf{m}_{pri}) \quad (1)$$

where the posterior pdf $\pi(\mathbf{m}_{\text{sec}},\mathbf{m}_{\text{pri}} \mid y)$ represents the updated knowledge about the subsurface lithologic and density distribution given the observed gravity data y. This quantity is proportional (up to a normalization constant c) to the product of the two prior pdfs, one considering the primary lithological subspace $\pi_p(\mathbf{m}_{\text{pri}})$ and a conditional pdf describing the dependence of the bulk density on the lithology $\pi_{s|p}(\mathbf{m}_{\text{sec}} \mid \mathbf{m}_{\text{pri}})$, and a likelihood function $L(y \mid \mathbf{m}_{\text{sec}})$, which quantifies probabilistically the misfit between the gravity potential field calculated from the joint model and the observed gravity data.

The aim of Bayesian inversion of gravity data is to infer the subsurface lithology and density distribution in light of gravity data and the prior geologic understanding of the system. Two types of geologic constraints are used to ensure that posterior results retain geologic meaning from the reference prior geologic model: 1) The preservation of vertical stratigraphic order, forcing model realizations to respect the vertical sequence of the stratigraphic units as specified in the reference prior geologic model; 2) A commonality criterion, which favors proposed model configurations in which stratigraphic units occupy similar positions as the reference prior geologic model In addition, the inversion process is not allowed to change the lithology of voxels that intersect the surface (the surface geologic map is unchanged by the inversion process). Unless otherwise noted, the lithology of voxels in the subsurface are not held constant during the inversion process. Thus, differential geological data quality is not considered and all voxels are equally uncertain. This contrasts with some other probabilistic geologic modeling schemes (Wellmann et al., 2017; de la Varga et al., 2019), which directly invert for the contact point and orientation measurements controlling the implicit interpolation.

The prior probability space implied by the reference prior geologic model and the assumed geologic constraints can be investigated using 'prior-only' inversion tests, which generate samples from the prior distribution without consideration of geophysical likelihoods. These tests show that the reference prior model exerts a strong influence on the probability space implied by the reference prior model even in the absence of any geologic constraints. Further, by enforcing the preservation of vertical stratigraphic relationships from the reference prior model in accepted model realizations, stratigraphic units can not be created (e.g. basement intrusions in between hyaloclastite and lava flow units) but can be destroyed as the boundaries of over- and underlying stratigraphic units change position. The probability of a proposed model configuration as a function of how closely it resembles the reference prior model (commonality misfit) is quantified using a Weibull distribution. The pdf for a Weibull distribution for a scale parameter λ and shape parameter κ is given as:

$$p\left(x\middle|\lambda,k\right)=\left(\frac{k}{\lambda}\right)\left(\frac{x}{\lambda}\right)^{k-1}\exp\left(-\left(\frac{x}{\lambda}\right)^{k}\right) \quad (2)$$

where x is the commonality misfit function. Assumption of a scale parameter of 0.5 implies an expected 67% overlap between the set of voxels defined for a particular stratigraphic unit in the reference model and those voxels in model realizations. A scale parameter of 0.05 implies a 95% overlap, and a scale parameter of 5 implies a 17% overlap. Figure 4a-c shows the prior probability of hyaloclastite along Section 1 when the shape parameter for the Weibull distribution is set to 0.05, 0.5, or 5 (corresponding to a tight, moderate or loose commonality constraint, respectively). The spatial distribution of prior probability more closely resembles the reference prior model when there is a tight commonality constraint. As the commonality constraint is loosened, the zones of intermediate probability along the edges of the stratigraphic units become more diffuse, increasing in width from 0.2-0.3 km to 0.5-0.7 km.

A Markov chain records a pseudo-random walk in a model space. To estimate the posterior probability density, three Markov chains are generated (Bosch, 1999; Bosch et al., 2001):

1. A primary chain for the lithological prior $\pi_p(\mathbf{m}_{pri})$
2. A prior chain, which samples from a joint pdf by using an outcome from the primary chain (a marginal pdf) to sample from the conditional pdf $\pi_{s|p}(\mathbf{m}_{sec} \mid \mathbf{m}_{pri})$
3. A posterior chain, which generates joint models of the lithology and density distribution constrained by the geophysical likelihood to evaluate $\pi(\mathbf{m}_{sec},\mathbf{m}_{pri} \mid y)$

The primary and posterior chain use a Metropolis sampling rule (Metropolis et al., 1953) to generate a chain ergodic to the primary and posterior pdf, respectively, considering the probability of a proposed model configuration as a function of commonality misfit in the primary pdf (eqn. 2) and the geophysical likelihood for the posterior chain (eqn. 1), similar to the framework described by Mosegaard and Tarantola (1995).

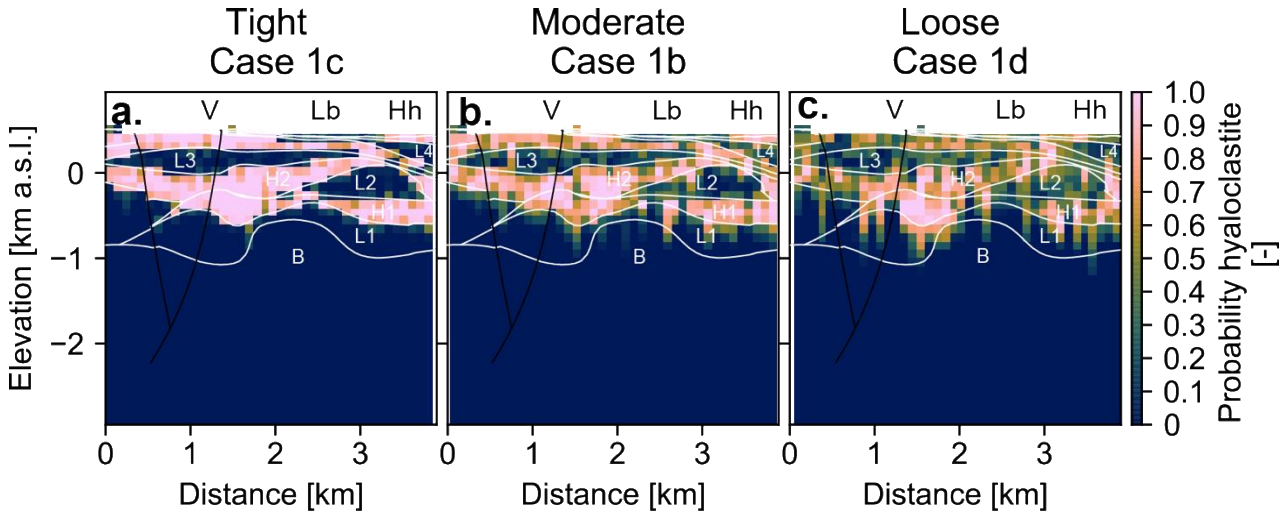

Figure 4. Prior-only results for lithology investigating effect of commonality constraint. Probability of hyaloclastite for inversion with a. tight b. moderate and c. loose commonality constraint (see text). Boundaries of the stratigraphic units and faults in the reference prior geologic model shown with white lines. Letters indicate proximity to different sub-areas of the Krafla field (V=Vitismor, Lb=Leirbotnar, Hh=Hvitholar).

The likelihood of a proposed model is calculated based on the misfit between the simulated gravity response of a proposed geologic model and the observed data. As described by Guillen et al. (2008), the likelihood is given by:

$$L(y\middle|\mathbf{m}_{sec}) = k\exp\left(\frac{\frac{1}{2}\sum_{l=1}^{N}[g_l(\mathbf{m}_{sec}) - y_l]}{\sigma^2}\right) \quad (3)$$

where k is a normalization factor, σ^2 is the variance of the data (i.e. measurement error), $g_l(\mathbf{m}_{sec})$ represents the modeled gravity field at the point of observation l while y_l represents the measurement of the gravity field at the same point, and N is the number of observations. Based on analysis of repeated gravity measurements at different stations and uncertainty of ~30 cm in the elevation measurements, the measurement error was assumed to be 0.1 mGal – this is likely a conservative value, in reality, and may be higher. According to the Metropolis rule, if the likelihood of a proposed model based on the calculated gravity response has a lower misfit with the measured dataset (higher likelihood) compared to the previous model, the proposed model is accepted and stored for determination of the posterior statistics. Otherwise, a proposed model is accepted with a probability given by its likelihood. For each inversion test considering geophysical likelihood (Case 2-5), fifteen million iterations were carried out. We assess convergence of the Markov chain on the basis of the calculated misfit between the forward modeled gravity field and observed data (calculated as

root mean square, RMS), and only store models for calculation of posterior statistics that have a misfit of less than 0.1 mGal. Model realizations with higher misfit are discarded as burn-in. The inversion process reduces the misfit to values of 0.1 mGal is reached within 1,000,000-2,000,000 iterations, after which point it is largely stable.

Proposed model configurations are generated by changing the density or changing the lithology (and thereby, the bulk density) of randomly selected voxels. One of the key parameters controlling the inversion process is the probability that changes to lithology are proposed. Maximum variability in lithologic structure is attained by setting the probability of lithologic changes to 100%, as is done for the 'prior-only' tests (Fig. 4). For the inversion runs including a commonality constraint and geophysical likelihood (Cases 3-5), the probability of lithologic changes is set to 50%.

3. RESULTS

3.1 Comparison between observed and calculated gravity field

A comparison between the observed and modeled gravity data is shown in Figure 5. The inversion process reduces misfit between the forward modeled gravity potential field and the measured data. Initially, the gravity field calculated using the reference prior model assuming mean properties for each rock type (Fig. 5b) predicts higher gravity values (6-12 mGal) than the observed data (Fig. 5a, 2-6 mGal). While the reference prior model with mean densities predicts lower gravity values in the SW between Leirbotnar and Vestursvæði, similar to the observed data, other anomalies in the mean data are not reproduced. After the inversion process, there is a close correspondence between the gravity field calculated for the changed model and the measured data (Fig. 5c). Note that Fig. 5c shows results at the end of an inversion run; the gravity field calculated varies slightly depending on the step in the inversion process and the run configuration. However, the absolute misfit values during the inversion process are nearly constant (0.1 mGal RMS), close to the uncertainty of the data, and generally similar between different model runs.

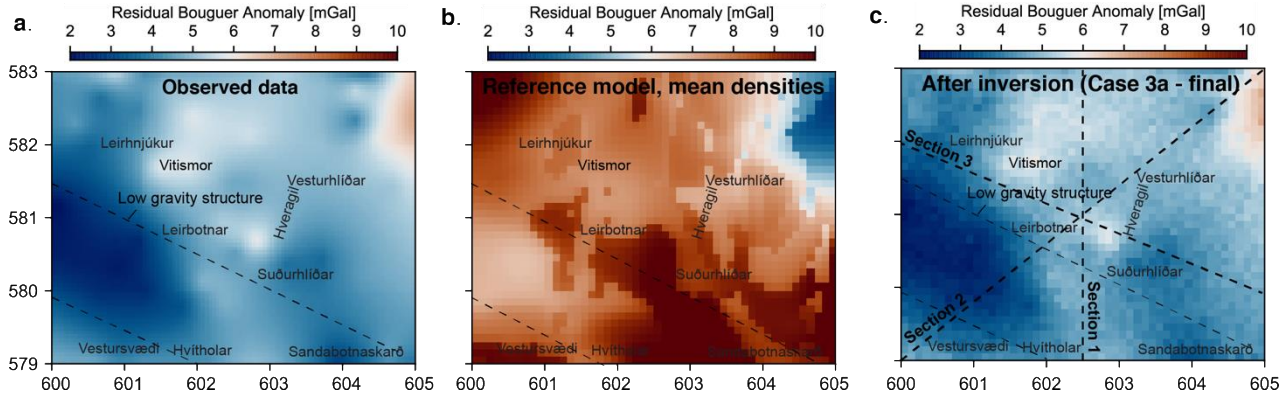

Figure 5. Comparison between observed and modeled gravity data. a. Observed Residual Bouguer anomaly in the model area b. Calculated residual Bouguer anomaly with reference prior geologic model assuming mean bulk densities for each type of lithology. c. Calculated residual Bouguer anomaly after inversion process.

3.2 Lithologic structure and bulk density distribution

The lithologic structure of the reference prior model is retained in the posterior results if a moderate commonality constraint is applied for the inversion process (Figure 6). The resemblance between the reference prior geologic model and posterior probability distributions for lithology is particularly strong in the upper 1.5 km, where the zones of intermediate probability along the boundaries of the lithologic units is of a similar or slightly lesser thickness (<0.2 km) as the prior-only tests. However, the reference prior geologic model and the posterior results for lithology differ insofar as the latter predicts a greater depth to basement intrusions, particularly beneath Vitismor, Hveragil and Leirbotnar (Fig. 6b,c,d). Viewing the posterior results for lithologic structure in terms of most probable lithology (Fig. 6g,h,i) also shows the similarities in the lithologic structure between the reference prior model and the posterior in the upper 1.5 km as well as the greater depth to basement intrusions predicted by the posterior results throughout most of the model domain.

Posterior results for the mass density distribution indicate a strong dependence on lithology, with the lowest values for mean bulk density values and highest values of the standard deviation of bulk density found within the hyaloclastite units. Figure 12 shows the spatial and depth distribution of mean bulk density (Fig. 6j,l,n) and the standard deviation of density (Fig. 6k,m,o) for an inversion with a moderate commonality constraint. Hyaloclastites show a low mean bulk density ~2.2 g cm^{-3}) and a high standard deviation of density (0.1-0.15 g cm^{-3}) compared to the higher density lava flows (~2.6 g cm g cm^{-3}) with a lower standard deviation of density (<0.1 g cm g cm^{-3}), and the basement intrusions with the highest mean bulk densities (~2.8 g cm g cm^{-3}) and lowest standard deviations (<0.05 g cm g cm^{-3}). Comparing the posterior results for bulk density to lithology, it can be seen that the relatively low mean bulk density (2.4-2.6 g cm^{-3}) and high standard deviation of density (<0.1 g cm g cm^{-3}) at >1.5-2 km depth beneath Leirbotnar is consistent with the high posterior probability of hyaloclastites occurring at such depths in this area.

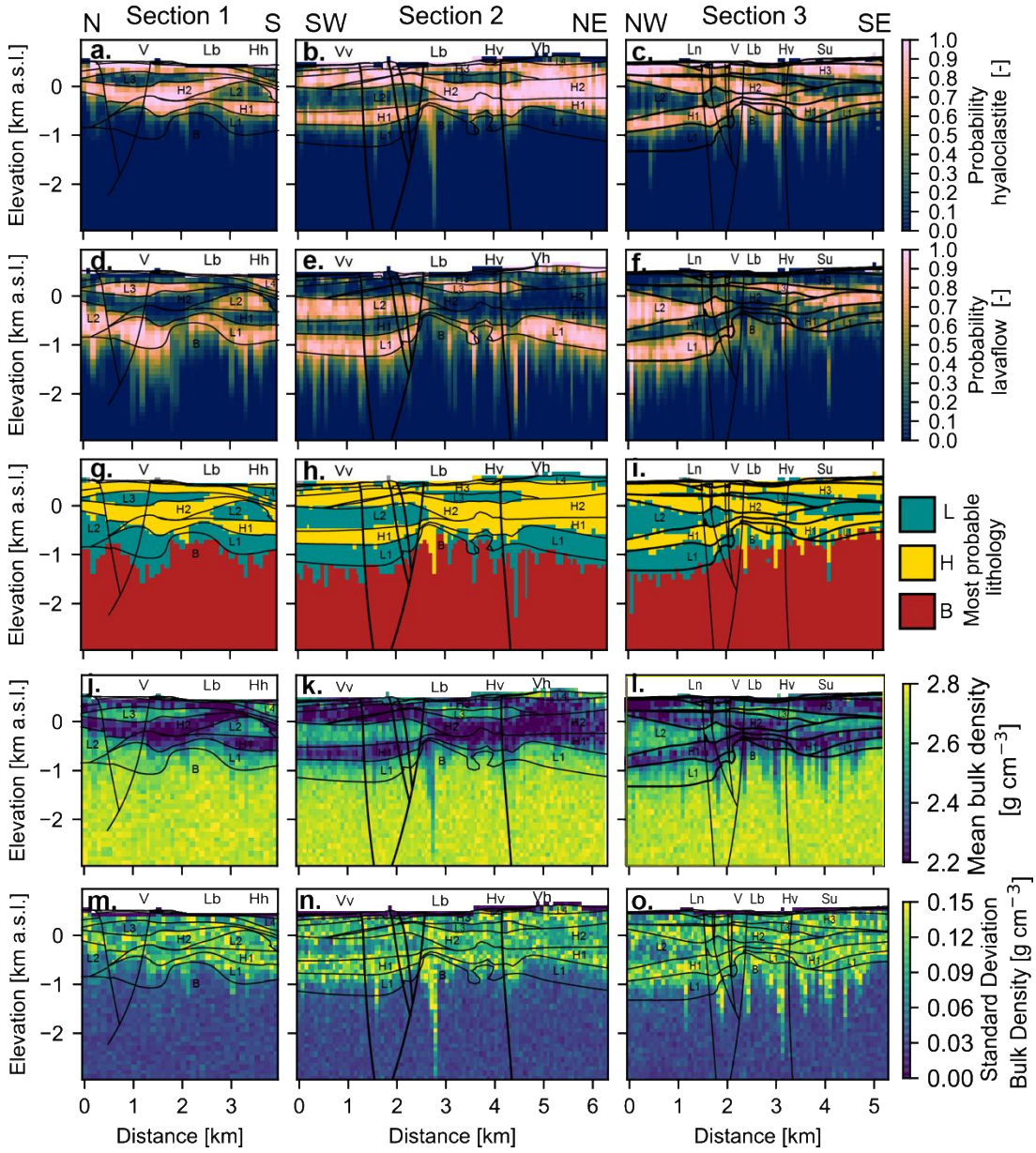

Figure 6. Posterior results for lithology for an inversion run with moderate commonality constraint. Posterior results for (a-c) probability of hyaloclastite, (d-f) probability of lava flow, and (g-i) most probable model. Results are shown along (a, d, g) Section 1, (b, e, h) Section 2, and (c, f, i) Section 3. Boundaries of the stratigraphic units and faults in the reference prior geologic model shown with black lines. Letters indicate proximity to different sub-areas of the Krafla field (V=Vitismor, Lb=Leirbotnar, Hh=Hvitholar, Hv=Hveragil, Vh=Vesturhlíður, Ln=Leirhnjúkur, Su=Suðurhlíður)

3.3 Uncertainty quantification

The uncertainty of model predictions depends on the strength of the geologic constraints imposed on the probabilistic inversions. For a discrete variable such as litho-type, the uncertainty of probabilistic geologic models can be quantified by the information entropy metric. For each voxel, the information entropy is given by:

$$H(x) = -\sum_{m=1}^{M} p_m(x)\log(p_m(x)) \tag{4}$$

where x denotes the location of the voxel and M the number of possible exclusive members (in this case, lithologies) the subregion can contain. The minimum entropy is 0, which indicates that a certain lithology has a probability 1 and that of all others is 0. The maximum entropy depends on the number of possible outcomes, and is found where the different possible lithologies are equally probable. The uncertainty of continuous variables such as bulk density can be characterized in terms of standard deviation.

The uncertainty of the reference prior geologic model, as specified by the strength of the commonality constraint, largely controls the magnitude of the information entropy and standard deviation of bulk density in the posterior results (Figure 7). However, although the uncertainty of the posterior results generally increases as the assumed uncertainty of the prior increases, certain regions of the

model show relatively high uncertainty even if a tight commonality constraint is assumed. Thus, the information entropy is close to zero at a distance of >0.2 km from the boundaries of the stratigraphic units if a tight commonality constraint is used, it increases to 0.3-0.4 along the top of the basement intrusions beneath Leirbotnar (Fig. 7b). For inversions with a moderate commonality constraint (Fig. 7d-f), lithologies have a substantial probability of occurring outside of the boundaries of the units specified in the reference prior model, so the information entropy is higher (0.45) and more widely distributed throughout the upper 2 km (less restricted to lithologic boundaries) and values near 0.3 extend to 0.5-1 km deeper than the depth of the basement as predicted by the reference prior model (Fig. 7e).

Inversions with a loose commonality constraint, (Fig. 7g-i) show larger zones of intermediate hyaloclastite probability (between 0.2-0.8) at depths less than 1 km b.s.l. (Fig. 7g), and the information entropy is >0.3 throughout much of the model (Fig. 7h). Although the magnitude and distribution of information entropy depends on the strength of the commonality constraint, all models predict relatively high information entropy in the top of the basement intrusions beneath Leirbotnar. By increasing the lithologic variability of the posterior, assuming a higher uncertainty of the reference prior geologic model also increases the uncertainty of the posterior bulk density distribution (Fig. 7c,f,i). For a tight commonality constraint, the standard deviation of bulk density only exceeds 0.1 g cm^3 along the boundaries of the hyaloclastite layers (Fig. 7c) and is lower in the lava flows and basement intrusions. However, values for the standard deviation of bulk density are higher (0.12-0.2 g cm^3) for inversion runs with a moderate (Fig. 7f) or loose (Fig. 7i) commonality constraint, and the areas with high density variability are more widely distributed throughout the upper 1.5-2 km and less confined to the hyaloclastite layers.

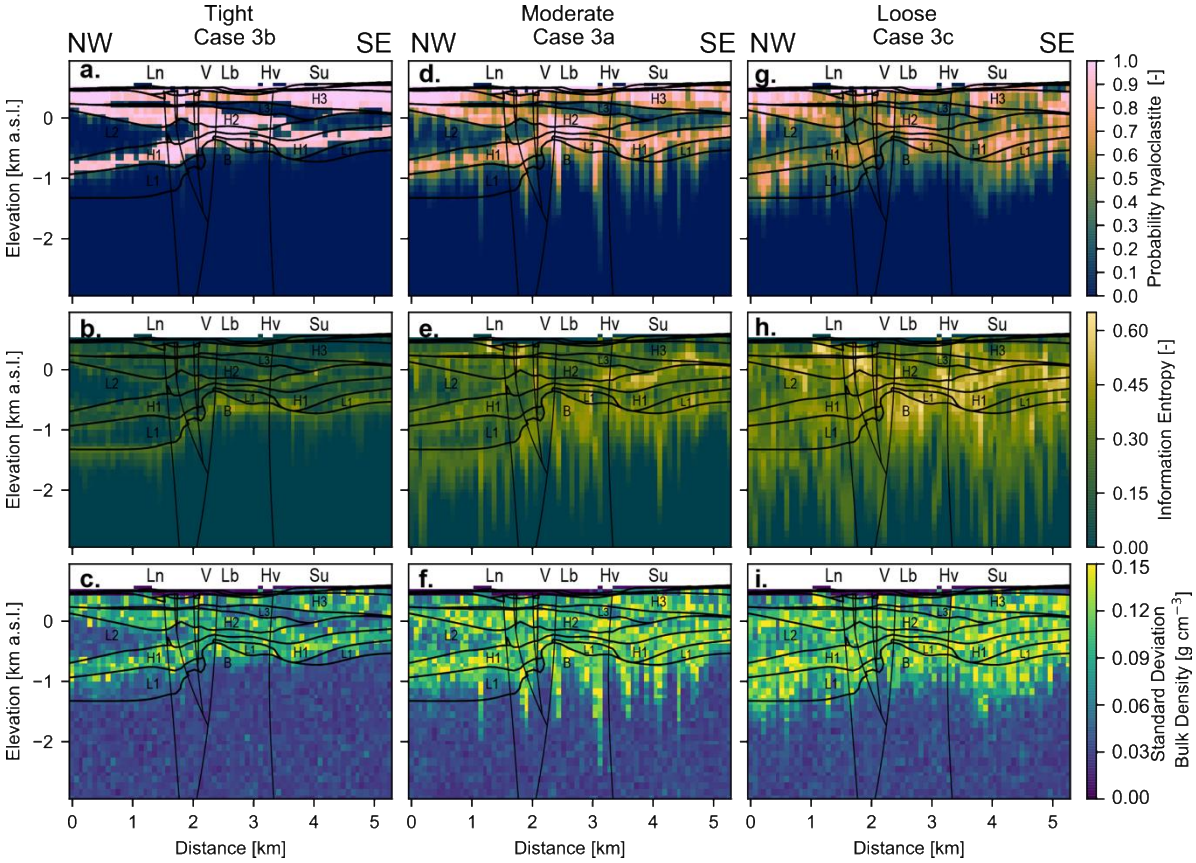

Figure 7. Effect of commonality constraint on posterior results for lithology and uncertainty quantification metrics. Posterior results for (a, d, g) probability of hyaloclastite and (b, e, h) information entropy, and (c, f, i) standard deviation of bulk density, for inversion runs with (a-c) tight commonality constraint, (d-f) moderate commonality constraint, (g-i) loose commonality constraint. Results are shown along Section 3.

4. DISCUSSION

4.1 Uncertainty of the prior

Bayesian inversion of gravimetric data requires the use of credible prior information in order to eliminate unreasonable models that may potentially fit the data. One of the major challenges of such inversion schemes is to specify the uncertainty of geologically complex prior information in such a way that still allows the inversion scheme to adequately explore the range of possible models that may be consistent with the data. While the prior probability density functions (pdfs) for the bulk density of each lithologic unit describe uncertainty in rock petrophysical properties, the reference prior geologic model represents only one possible model of the subsurface lithologic structure. Some approaches to probabilistic geologic modeling describe the uncertainty of the geologic prior in terms of prior pdfs for the contact point and orientation measurements, and invert directly for these measurements (Wellman et al., 2017; de la Varga et al., 2019). As the reference prior geologic model used in this study represents only an interpretation of the stratigraphic data, we take a different approach and invert for voxel lithology and bulk density.

We describe the uncertainty of the reference prior geologic model probabilistically through several inversion control parameters:1) the probability that the inversion scheme proposes lithologic changes to the reference prior model, or only proposes changes to voxel density, keeping lithology constant, 2) the strength of the commonality constraint, which expresses probabilistically the expected overlap between the lithologic structure of model realizations and the reference prior model, 3) the voxel resolution, which determines how finely the model domain is discretized into blocks of uniform lithology and density. The uncertainty of reference prior geologic model of Krafla is partially due to a scarcity of data, but is also due to the challenge of correlating stratigraphic measurements between wellbores in systems containing hyaloclastites, which form mountain and ridges rather than layers of near-constant thickness. Although the reference prior geologic model does not resolve such fine-scale lithologic complexity, the distribution of posterior probabilities for each lithology assuming a moderate commonality constraint suggests that the simplified reference prior model may be consistent with the gravity data. However, the observed correspondence between the posterior results and the reference prior geologic model is largely a result of the imposed commonality constraint. That *a priori* beliefs about the uncertainty of the reference prior model exert such a strong influence on posterior results is seemingly at odds with the philosophy of Bayesian inversion, which aims to condition uncertain beliefs based on observed data. A non-informative prior (without the commonality constraint or with a very loose commonality constraint) results in an overly broad, geologically meaningless suite of models that may be consistent with the data.

By expressing the uncertainty of the geologic prior probabilistically through the commonality constraint and varying this uncertainty between inversion runs, we can investigate how posterior results begin to deviate from the reference prior model as the confidence of the prior model is reduced. This may allow us to infer where the reference prior model is most uncertain, in the sense that it is most likely to contradict the observed gravity data. If the inversion proposes lithologic changes to the reference prior model without consideration of commonality or with a loose commonality constraint, lithologic boundaries migrate far (>1 km) from their positions in the reference prior model during the inversion process. The use of a tight commonality constraint results in a posterior model for lithology that closely resembles the reference prior model and is similar to a 'density-only' inversion with a deterministic geologic prior. Since the uncertain zones are only restricted to the edges of the stratigraphic units, this likely underestimates the uncertainty of the subsurface structure.

A moderate strength commonality constraint preserves the resemblance to the geologic prior model in the results for posterior lithologic structure, while also allowing divergence between the prior and posterior in areas where the prior model may be inconsistent with the gravity data and may thus need to be altered. Figure 8 compares the most probable lithologic models for the three inversion runs using a moderate commonality constraint: 1) a base-case scenario (similar to Figure 6); 2) the same reference prior geologic model but with the bulk density of the hyaloclastite units increased to account for the effects of alteration; and 3) a prior reference geologic model that includes a rhyolitic intrusion in the vicinity of Vitismor (consistent with the evidence from the Iceland Deep Drilling Project IDDP-01 well, which encountered a shallow intrusion in the vicinity beneath this area). The most probable lithologic models resemble one another and the reference prior model throughout the upper 1 km of the model. The divergence between the posterior probability results for lithology and the lithologic structure of the reference prior model is greatest beneath Leirbotnar, Vitismor and Hveragil, where the inversion results predict basement intrusions restricted to depths >1 km b.s.l., roughly 0.5 km deeper than described by the reference model. Further, the zone with a high probability of hyaloclastites between 1-1.5 km depth b.s.l. expands laterally and to greater depths if the prior pdfs for the bulk density of the hyaloclastite units are set to higher values to reflect the effects of high-temperature rock alteration. Additionally, the discrepancy in the posterior results remains if the lithologic structure of reference prior model is altered to include a low-density rhyolitic intrusion at depth beneath this area.

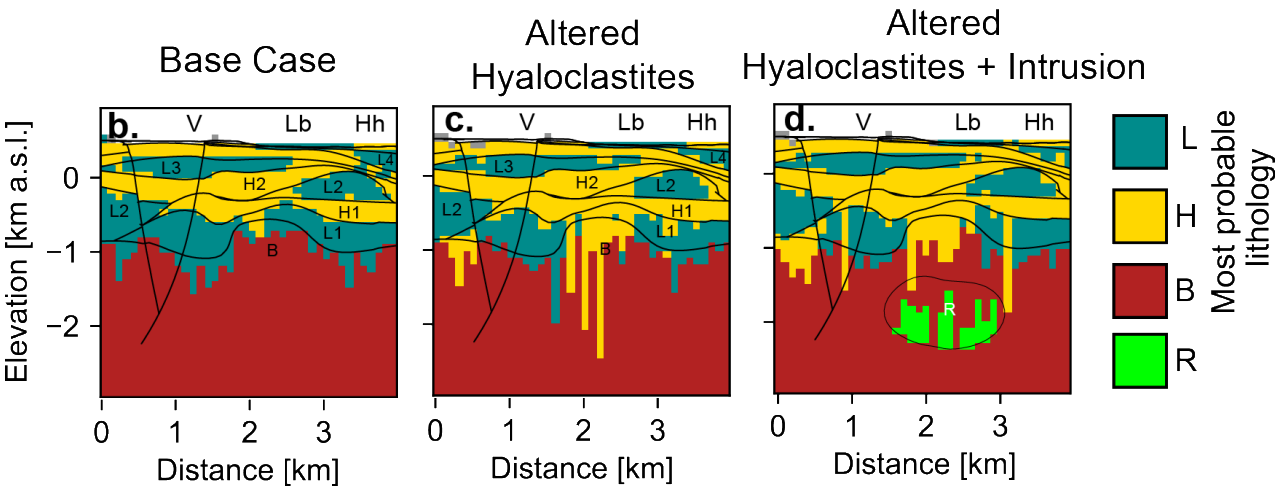

Figure 8. Comparison of posterior results for different inversion runs. See text for description of different inversion runs.

The reason for the narrow region of deeper hyaloclastites predicted by the inversion in this area is because the measured Bouguer anomaly is too low to be consistent with the shallow depth of basement intrusions described by the 'base-case' reference prior geologic model. Since the high density basement intrusions at depths of 1-2 km b.s.l. result in a too high positive gravity anomaly, lower mass densities are required in this area for the model to be consistent with the observed data. The stratigraphic data from several wells drilled in this area indicates basaltic intrusions at depths >1 km b.s.l. as well as extrusive lava flows and rhyolitic intrusions such as granophyre and felsites interspersed within the basement intrusions (Mortensen et al., 2009). Thus, specifying the lithology of this area as basement intrusions in the reference prior model may be an oversimplification. The inversions with a moderate commonality constraint that include a low-density rhyolitic magma chamber in the reference prior model only predict a high probability of rhyolitic magma at depths >2 km b.s.l., roughly 0.5 km deeper than encountered in the IDDP-1 well and well KG-39

(Elders et al., 2014). Although the density of this magma is not known, the density of rhyolite assumed in the prior pdf (2.3 ± 0.1 g cm^{-3}) is based on laboratory measurements (Bagdassarov and Dingwell, 1994) and may be an underestimation. Low fluid densities associated with vapor-rich boiling zones or supercritical fluids near the intrusion may also explain the low mass density predicted in this area.

4.2 Inferred density structure

The posterior probabilities for bulk density depend on the lithology-specific prior physical property pdfs as well as the geologic constraints imposed on the inversion process. In these inversions, a posterior pdf for bulk density is defined for each voxel (e.g. Fig. 6). The impact of the inversion runs on the posterior probabilities for bulk density can be assessed on the basis of litho-type by grouping voxels according to the lithology specified by the 'most probable' model. Calculated in this way, the posterior results for hyaloclastites are particularly sensitive to the specified prior pdf for bulk density and the reference prior geologic model. Figure 9 shows that the uncertainty of the bulk density of each rock type is reduced by the inversion process, but the posterior results for the bulk density of each litho-type depend on the assumed geologic constraints assumed during the inversion process as well as the prior pdfs. In the an inversion runs with very tight geologic constraints (i.e. a density-only inversion), the lowest densities for hyaloclastites are predicted. For the runs with the reference prior geologic model and a moderate commonality constraint constraints, posterior bulk densities are slightly higher than the prior mean. Higher bulk densities for hyaloclastite if the prior pdf is changed to reflect the effects of alteration or if the geologic model includes a low density intrusion. These results indicate that when the prior geologic constraints are loosened, higher bulk densities are predicted for hyaloclastites.

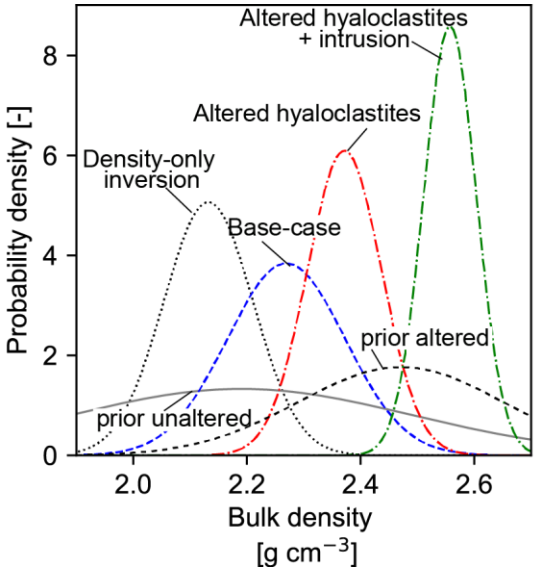

Figure 9. Comparison of posterior results for bulk density of hyaloclastite for different inversion runs (see text). Normal distributions for each rock type and inversion run are calculated with voxels grouped according to most probable lithology.

The sensitivity of the posterior results for hyaloclastite bulk density to the assumed geologic constraints suggests that this lithology plays a key role in controlling the gravity response of the geologic model, particularly the ESE-WNW trending gravity low partially located in the southern part of the geologic model. Figure 10 shows the thickness of hyaloclastites according to the most probable model (Figure 10a-b) and the mean bulk density of hyaloclastites (Fig. 10c-d), calculated by averaging the mean bulk densities of all voxels in a vertical column of the model grouped as hyaloclastite according to most probable model. The thickness of hyaloclastites depends on the inversion run, with thicker hyaloclastites predicted by the inversion runs with higher assumed prior bulk density for hyaloclastites. However, the most probable model predicts thicker hyaloclastites in the in area of Leirbotnar/Sudurhlidur/Hveragil (1.2-1.8 km), and lower thicknesses (<1 km) in the southern part of the field where the ESE-WNW oriented gravity low is located. While the mean bulk density of hyaloclastite viewed depends on the inversion run, bulk densities are generally higher in the area of Leirbotnar, and lower in the northwest of the model as well as a significant part of southern part of the field. Moreover, in the southern part of the model, the zone with relatively low density hyaloclastites follows the boundary of the low gravity zone. These results seem to indicate that a relatively low hyaloclastite density may be an explanation for the ESE-WNW-trending gravity low.

Previous models for the ESE-WNW-trending gravity low (Árnason et al., 2007) have focused on the greater thickness of hyaloclastite in this area (Ármannsson et al., 1987). That our results don't predict the thickest hyaloclastites in the area of the ESE-WNW-trending gravity low is related to the discrepancy between the prior model and the posterior results for lithology described above, and the low expected mass densities in the central part of the field. However, as indicated by the rock alteration data, hyaloclastite density in the south could be an indication of a relatively low abundance of epidote-chlorite facies altered hyaloclastite. In this case, the gravity low may indicate a buried transverse fault with an ESE-WNW orientation (similar to the Husavik Flatey Fracture Zone transform zone to the north, Fig. 1b) that compartmentalizes fluid flow in the Krafla reservoir. The notion of a ESE-WNW-oriented bounding fault in this area is also supported by the near-ESE-WNW alignment of hot springs along the southern margin of the central part of the field (Figure 1) as well as the resistivity structure of the system, which suggests that the shallow low-resistivity cap rock does not extend into the area of the transverse gravity low structure, supporting the notion that the hyaloclastites in this area are relatively unaltered.

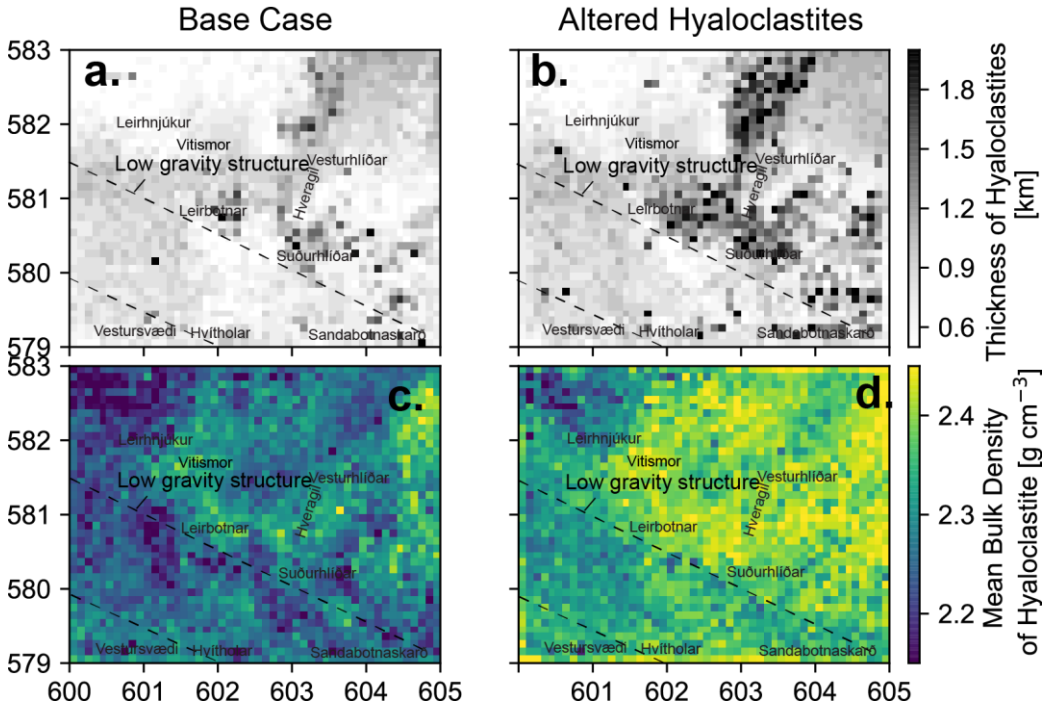

Figure 10. Comparison of thickness of hyaloclastite and mean bulk density of hyaloclastites for base-case inversion run and inversion run with prior pdf for hyaloclastites reflecting the effects of alteration.

5. CONCLUSIONS

This study presents a suite of probabilistic geologic models of the Krafla geothermal system constrained by measured gravity data. We combine a reference prior geologic model built from borehole data and statistical analysis of rock properties in a Bayesian inference framework to generate a probability distribution for the distribution of major lithologies and subsurface density distribution. This study investigates how varying the uncertainty of the prior affects posterior probabilities and uncertainty quantification metrics obtained by probabilistic, litho-constrained inversion of gravity data. For geologically complex systems such as volcano-hosted geothermal systems, knowledge of the structure and properties of the subsurface is not exact. More broadly, even the uncertainty of this knowledge is not very well known. Yet this uncertainty must be specified in the prior, both through the imposed geologic constraints, such as the commonality constraint, and the prior physical property distributions for each lithology. While rock petrophysical properties are measured in the lab may be known with some confidence, there is uncertainty stemming from changes in rock properties of rock samples between the surface and depth. However, the greater uncertainty lies with the geologic structure.

This study underscores that use of a probabilistic approach to geophysical inversion is not a silver bullet for avoiding the non-uniqueness problems associated with inversion of potential field data such as gravity data, and that "classical" geologic studies and laboratory measurements of rock properties play key roles in developing reasonable prior constraints for such inversions. Inversions with different prior reference geologic models and/or prior physical property distributions result in different 'most probable' models, all of which match the observed data. Although posterior results are better thought of in terms of probabilities instead of most probable model, the point remains that meaningful posterior results depend on having a reliable prior model for geologic structure. Thus, conventional geologic studies (mapping, lithologic analysis, correlation of stratigraphic measurements between boreholes) play an essential role in developing a meaningful prior that can be used for Bayesian inversion of geophysical data. This requirement may limit the utility of Bayesian inference techniques for systems for which only very little geologic data is available.

ACKNOWLEDGEMENTS

We thank Ingvar Thor Magnusson for sharing the gravity data, helpful discussion with Knutur Arnason, Annette Mortsensen, and Nataly Castillo-Ruiz. This paper is funded by Rannis Technology Development Fund.

REFERENCES

Abdelfettah, Y., Schill, E. and Kuhn, P.: Characterization of Geothermally Relevant Structures at the Top of Crystalline Basement in Switzerland by Filters and Gravity Forward Modelling. *Geophys. J. Int.*, **199**, (2014), 226–241.

Altwegg, P., Schill, E., Abdelfettah, Y., Radogna, P. V. and Mauri, G.: Toward Fracture Porosity Assessment by Gravity Forward Modeling for Geothermal Exploration (Sankt Gallen, Switzerland). *Geothermics*, **57**, (2015), 26–38.

Ármannsson, H., Guðmundsson, Á., and Streingrímsson, B.: Exploration and development of the Krafla geothermal area. *Jökull*, **37**, (1987), 13-30.

Árnason, K., Vilhjálmsson, A., and Björnsdóttir, Þ.: A Study of the Krafla Volcano using Gravity, Micro-Earthquake and MT data. *KenGen, Lake Naivasha, Kenya*, (2007).

Bagdassarov N. and Dingwell D. (1994) Thermal properties of vesicular rhyolite. *J. Volcanol. Geotherm. Res.* **60**, 179–191.

Boulanger, O. and Chouteau, M.: Constraints in 3D Gravity Inversion. *Geophys. Prospect.* **49**, (2001), 265–280.

Bosch, M.: Lithologic Tomography: From Plural Geophysical Data to Lithology Estimation. *J. Geophys. Res. Solid Earth* **104**, (1999), 749–766.

Bosch, M., Guillen, A. and Ledru, P.: Lithologic Tomography: An Application to Geophysical Data from the Cadomian Belt of Northern Brittany, France. *Tectonophysics* **331**, (2001), 197–227.

Caers, J.: *Modeling Uncertainty in the Earth Sciences*, John Wiley & Sons, West Sussex, UK (2011)

Calcagno, P., Chilès, J.P., Courrioux, G., and Guillen, A.. Geological Modelling from Field Data and Geological Knowledge: Part I. Modelling Method Coupling 3D Potential-Field Interpolation and Geological Rules. *Physics of the Earth and Planetary Interiors*, 171, (2008), 147–57.

Chen, J., Hoversten, G.M., Key, K., Nordquist, G. and Cumming, W.: Stochastic Inversion of Magnetotelluric Data using a Sharp Boundary Parameterization and Application to a Geothermal Site. *Geophysics*, **77**, (2012), E265–E279.

Corbel, S., and Wellmann, F.: Framework for Multiple Hypothesis Testing Improves the Use of Legacy Data in Structural Geological Modeling. *GeoResJ*, **6**, (2015). 202–212.

Covell, C.D, Valfells, A., Guðjónsdóttir, M.S., Stefánsson, H., Julíusson, E., and Pálsson, H. "Data Fusion for Hydrothermal Reservoir Characterization through Use of Bayesian Statistical Inference and MCMC Maximum Likelihood Models." *Proceeding*, : Forty-Second Workshop on Geothermal Reservoir Engineering, Stanford University, Stanford, CA, (2017).

de la Varga, M., Schaaf, A. and Wellmann, F.: GemPy 1.0: Open-Source Stochastic Geological Modeling and Inversion. *Geosci. Model Dev.* **12**, (2019).

de la Varga, M., Wellmann, F. and Murdie R. "Adding Geological Knowledge to Improve Uncertain Geological Models: A Bayesian Perspective." *Geotectonic Research*, 97, (2015), 18–20.

Elders, W.A., Friðleifsson, G.Ó. and A. Albertsson: Drilling into Magma and the Implications of the Iceland Deep Drilling Project (IDDP) for High-Temperature Geothermal Systems Worldwide, *Geothermics*, **49**, (2014), 111–118.

Franzson H., Gudlaugsson, S., and Fridleifsson, G.O.: Petrophysical properties of Icelandic rocks. *Proceedings*, Sixth Nordic Symposium on Petrophysics, Trondheim, Norway. (2001)

Franzson, H., Gudfinnsson, G. and Helgadottir, H.: Porosity, Density and Chemical Composition Relationships in Altered Icelandic Hyaloclastites. *Water-Rock Interaction*, **13**, (2010)

Franzson, H., Gudfinnsson, G.H., Frolova, J., Helgadóttir, H., Mortensen, A.K. and Jakobsson S.P. *Icelandic Hyaloclastite Tuffs*. Tech. Rep., ISOR-2011/064, (2011)

Frolova, J.V., Ladygin, V.M., Franzson, H., Sigurðsson, O., Stefánsson, V. and Shustrov, V.: Petrophysical Properties of Fresh to Mildly Altered Hyaloclastite Tuffs. *Proceedings*, World Geothermal Congress, Antalya, Turkey, (2005).

Fullagar, P. K., Pears, G. A. and McMonnies, B.: Constrained Inversion of Geologic Surfaces—Pushing the Boundaries. *Leading Edge*, **27**, (2008), 98–105.

Guillen, A, Calcagno, P., Courrioux, G., Joly, A., and Ledru, P. Geological Modelling from Field Data and Geological Knowledge: Part II. Modelling Validation Using Gravity and Magnetic Data Inversion. *Physics of the Earth and Planetary Interiors*, **171**, (2008), 158–169.

Intrepid Geophysics: *3D GeoModeller Reference*, (2017a)

Intrepid Geophysics: *Forward Modeling and Inversion with 3D GeoModeller*, (2017b)

Jessell, M., Aillères, L. De Kemp, E., Lindsay, M., Wellmann, F. Hillier, M., Laurent, G., Carmichael, T., and Martin, R. "Next Generation Three-Dimensional Geologic Modeling and Inversion." *Society of Economic Geologists - Special Publications*, 18, (2014), 261–72.

Johnsen, G.V, Bjornsson, A. and Sigurdsson S.: Gravity and elevation changes caused by magma movement beneath the Krafla caldera, northeast Iceland. *Journal of Geophysics*, **47**, (1980), 132–140.

Johnsen, G.V.: (Gravity map of the Krafla area). *Eyjar í eldhafi: Reykjavík, Gott mál hf*, (1995), 93-100.

Kristmannsdóttir, H. Alteration of Basaltic Rocks by Hydrothermal Activity at 100-300 C, *Developments in Sedimentology*, 27, (1979), 359-367.

Li, Y. and Oldenburg, D. W.: 3-D Inversion of Gravity Data. *Geophysics* **63**, (1998), 109–119.

Magnússon, I.Þ.: Gravity Measurements at Theistareykir in July-September 2015 and Gravity Map of the Krafla Area. Tech. Rep. (Report in Icelandic), *Iceland GeoSurvey*, (2016), LV-2016-090.

McCalman, L., O'Callaghan, S.T., Reid, A., Shen, D., Carter, S., Krieger, L., Beardsmore, G.R., Bonilla, E.V. and Ramos, F.T.: Distributed Bayesian Geophysical Inversions. *Proceedings*, Thirty-Ninth Workshop on Geothermal Reservoir Engineering, Stanford University, Stanford, CA (2014).

Metropolis N., Rosenbluth, A.W., Rosenbluth, M.N., Teller, A.H. and Teller, E.: Equation of State Calculations by Fast Computing Machines. *J. Chem. Phys.*, **21**, (1953), 1087–1092.

Miller C.A., Williams-Jones G., Fournier, D. and Witter, J.: 3D Gravity Inversion and Thermodynamic Modelling Reveal Properties of Shallow Silicic Magma Reservoir Beneath Laguna del Maule, Chile. *Earth Planet. Sci. Lett.* **459**, (2017), 14–27.

Mortensen, A.K., Gudmundsson, Á., Steingrímsson, B., Sigmundsson, F., Axelsson, G., Ármannsson, H. et al. The Krafla Geothermal Field. Overview of Geothermal Research and a Revised Conceptual Model. (Report in Icelandic). *Iceland GeoSurvey. ÍSOR-2009/057.* (2009).

Mosegaard, K., and Tarantola, A.: Monte Carlo Sampling of Solutions to Inverse Problems. *Journal of Geophysical Research: Solid Earth*, 100.B7, (1995), 12431-12447.

Saemundsson, K.: Krafla. Geologic Map, 1:25000. Technical Rep., Landsvirkjun and Iceland GeoSurvey, Reykjavik, Iceland (2008)

Scales, J.A. and Tenorio, L.: Prior Information and Uncertainty in Inverse Problems. *Geophysics,* **66**, (2001), 389–397.

Sæmundsson, K. *Krafla geothermal map, 1:25000.* Reykjavík: Landsvirkjun and ÍSOR. (2008).

Weisenberger, T.B., Axelsson, G., Arnaldsson, A., Blischke, A., Óskarsson, F., Ármannsson, H., Blanck, H., Helgadóttir, H.M., Berthet, J-C., Árnason K., Ágústsson, K., Gylfadóttir, S., and Guðmundsdóttir, V.: Revision of the Conceptual Model of the Krafla Geothermal System. *Iceland GeoSurvey*, ÍSOR-2015/012; LV-2015-040 (2015).

Wellmann, J. F., Horowitz, F.G., and Regenauer-Lieb, K.: Towards a Quantification of Uncertainties in 3-D Geological Models, *Proceedings,* International Association for Mathematical Geosciences, University of Salzburg. Salzburg, Austria. (2011).

Wellmann, J. F., de la Varga, M., Murdie, R. E., Gessner, K., and Jessell, M. "Uncertainty estimation for a geological model of the Sandstone greenstone belt, Western Australia–insights from integrated geological and geophysical inversion in a Bayesian inference framework." *Geological Society, London, Special Publications*, *453*, (2017), SP453-12.

Witter, J.B., Siler, D.L., Faulds, J.E. and Hinz, N.H.: 3D Geophysical Inversion Modeling of Gravity Data to Test the 3D Geologic Model of the Bradys Geothermal Area, Nevada, USA. *Geothermal Energy* **4,** (2016).